Binding energies and dissociation pathways in the aniline-Ar_2 cation complex

Quanli Gu and J. L. Knee[a)]
Department of Chemistry, Wesleyan University, Middletown, Connecticut 06459, USA

(Received 31 October 2007; accepted 29 November 2007; published online 11 February 2008)

Mass analyzed threshold ionization spectroscopy is used to measure the Ar binding energy for the cationic aniline-Ar (An^+-Ar) and aniline-Ar_2 (An^+-Ar_2) complexes. Since the experiments begin with the neutral species, photoexcitation creates the cations in the π-bonding configuration with the Ar located above the phenyl ring. The binding energy in this conformation of the An^+-Ar complex is determined to be 495 ± 15 cm^{-1}. Measurements of An^+-Ar_2 revealed the production of a lower energy dissociation product which is assigned to the An^+-Ar H-bonding configuration. Combinations of measurements allow determination of the dissociation energy of this complex to be 640 ± 20 cm^{-1}. The observation of a more stable H-bonded conformer is consistent with recent infrared experiments on An^+-Ar complexes created by complexing An^+ with Ar, rather than creation through the neutral complex. Calculations are presented which closely reproduce the binding energy of the π bound Ar but underestimate the stability of the H-bonded species.
 [DOI: 10.1063/1.2827458]

I. INTRODUCTION

The structure, energetics, and dynamics of van der Waals clusters have been an intense area of study for many years. One of the interesting features is the possibility for multiple, relatively low lying, structural minima. Of particular recent interest is the relative importance of π bonding compared to hydrogen bonding configurations which are of interest in biological molecules.[1,2] The aniline-Ar (An–Ar) complex has the possibility for both types of bonding. In the neutral complex π bonding is the most stable[3–5] interaction, whereas in the cation complex the H-bonding configuration appears to dominate.[6,7]

The presence of multiple minima is sometimes revealed by spectroscopic measurements, but often these measurements are not sensitive to the multiple minima or the techniques used to create the complexes do not provide access to all structures. One area where this is particularly true is in the study of cation complexes. Cation complexes have been studied quite extensively using primarily two types of experimental techniques. The first is photoelectron spectroscopy (PES) where the cation complexes are studied starting with the neutral complex, often using resonant excitation, through intermediate neutral states to ultimately probe the cation complex. Zero electron kinetic energy (ZEKE) spectroscopy[8] and the related mass analyzed threshold ionization (MATI) techniques[9–11] have been the most important techniques for measuring these PESs. The second prominent approach to the study of cation complexes is photofragmentation spectroscopy. In these techniques the transition in the cation is measured using action spectroscopy in which the absorption leads to fragmentation of the complex which is easily measured via mass spectroscopy.[6,7,12–14] Spectra can be measured in the IR, visible, and UV portions of the spectra with the only limitation being that photon absorption must lead to complex dissociation, a condition easily met in these weakly bound systems. The preparation of cation complexes can be done either by starting with the cation monomer and forming the cation complex directly in the expansion,[6,7] or alternatively by creating the cation complex via photoionization of the neutral species.[2,6] As is known, and demonstrated below these two approaches do not always prepare the same complex structures.

van der Waals molecules containing aniline as a chromophore have been a very well studied group of molecules with a wide variety of experimental and theoretical methods applied.[3,5,12,15–20] The cation complexes have also been extensively studied using both the photoelectron[18] and photofragmentation[6,7,12] approaches mentioned above. Our group did a significant amount of work on $An-Ar_n$ and $An-CH_4$ both on the neutral complexes using resonance enhanced multiphoton ionization (REMPI) and the cation complexes using ZEKE spectroscopy.[17,18] In this work, we have extended the studies of these systems using MATI spectroscopy to measure the binding energies of several conformations of An–Ar and $An-Ar_2$. Krause and Neusser[21] showed that MATI spectroscopy of clusters can be used to accurately measure the binding energy of cation complexes, and then, from the spectral shifts, extrapolate these values to obtain the binding energies in the S_1 and neutral ground state S_0. We applied these methods to aniline-Ar_n complexes ($n=1$ and 2) and found an anomalous result for $n=2$.

II. EXPERIMENTAL

Several types of spectroscopy have been applied to study aniline-$Ar_{1,2}$ in the first excited S_1 state and the cation ground state D_0. The S_1 spectrum was measured using mass resolved REMPI spectroscopy. The ionic ground states were

[a)]Author to whom correspondence should be addressed. Electronic mail: jknee@wesleyan.edu.

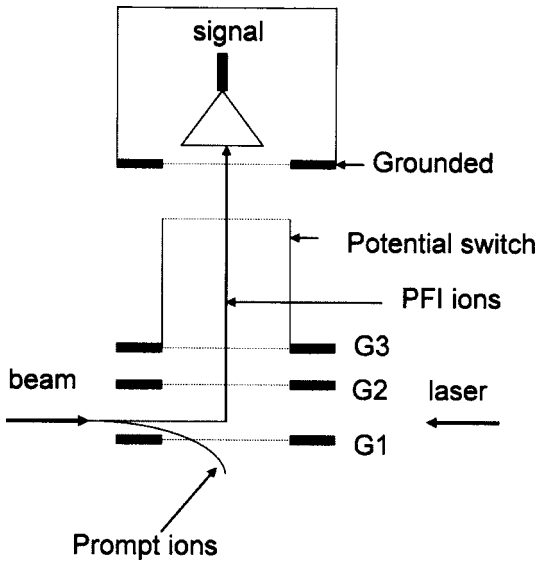

FIG. 1. Schematic illustration of the MATI detection apparatus. Total distance from G1 to detector is ~20 cm, spacing of G1 and G2 is 1.4 cm, and G2 to G3 spacing is 0.5 cm. See text for details.

studied using MATI spectroscopy.[9] The following describes the experimental apparatus which is presented more completely in previous publications.[11,22]

Aniline was obtained from Aldrich and used without further purification. It was heated to 50 °C in the sample container of a pulsed nozzle (General Valve). This nozzle, located in a differentially pumped molecular beam apparatus, produces a supersonic expansion using He/Ar mixtures as the buffer gas at a total pressure of 2 bars. The percentage of argon in the mixture was typically 10% but several of the experiments used pure Ar. The resulting molecular beam is skimmed before entering the second chamber, where REMPI and MATI spectroscopies take place.

Two independently tunable ultraviolet laser pulses are used in the experiments. The probe laser is a pulsed nanosecond Nd:YAG (YAG denotes yttrium aluminum garnet) operating at 20 Hz (Lumonics NY-61), pumping a tunable dye laser (Lumonics HD500) with a visible bandwidth of 0.05 cm^{-1}. The visible output of this laser is frequency doubled (Spectra-Physics WEX) and provides approximately 1 mJ/pulse in the UV. The pump laser system is also a Nd:YAG (Quanta-Ray GCR-3) pumping a tunable dye laser (Quanta-Ray PDL) equipped with frequency doubling capabilities (Spectra-Physics WEX). These two lasers are spatially overlapped in the interaction region: One functioning as the pump laser and the other as the probe. The temporal overlap of the lasers is controlled by a digital pulse generator (Stanford Research Systems, DG535) and adjusted to optimize the two-color dependent signal.

The mass spectrometer and MATI detection scheme are revised from previous published work and so will be described more fully. Figure 1 shows a schematic representation of this portion of the apparatus. The pump and probe lasers are combined with a dichroic mirror and mildly focused with a 1 m lens and counterpropagated on the axis of the molecule beam. The ion detection configuration we use now is more compact, with a total flight tube length of only 20 cm. For MATI experiments excitation occurs in field free conditions between grids G1 and G2 but quite close to G1 (1–2 mm). After a delay of ~100 ns (Ref. 23), a small discrimination voltage pulse (+1 V) is applied to G2, which is used to separate any prompt ions from high Rydberg states which may have been created. Under the influence of this discrimination field, and given sufficient time (20–50 μs), the prompt ions pass through grid G1 and thus are eliminated from detection. After this delay time a high-voltage, fast rise time, positive pulse is applied to G1 (+1100 V, Directed Energy, Inc.) which field ionizes any remaining high Rydberg states and accelerates the resulting ions to the detector. Simultaneous with this pulse, a second pulse is applied to grid G3, with an amplitude of −3300 V. The combination of voltages on G1 and G3, along with the near 0 V potential of G2, gives the Wiley-McLaren[24] space focusing parameters required for well resolved mass peaks at the detector. Grid G3 is not simply a grid but is actually a cylinder of length 4 cm, with mesh on the entrance and exit sides, which acts as a potential switch. During the time the ions of interest traverse this cylinder, the voltage is switched back to zero, thus allowing for normal detection by the microchannel plate detector with a face voltage of −2300 V and the anode at ground potential. We have found that this pulsed extraction arrangement leads to mass peaks of ~4 ns width at 100 amu, which yields excellent mass resolution even with the short flight time (~3.5 μs). The overall pulsed extraction, with the potential switch, is somewhat complicated but it has the advantage of keeping grid G2 always at low voltage (0 or +1 V), thus making control of the discrimination pulse much easier and more precise.

Data collection is performed using digital capture of the ion arrival signal (HP 54510A oscilloscope). After signal averaging for eight laser shots, the oscilloscope data are transferred to a computer and the entire mass spectrum is stored as a function of wavelength. The laser wavelength scans are computer controlled and the resulting spectrum in the appropriate mass channels is constructed from the full data set.

III. RESULTS

Figure 2 shows the S_1 spectra of aniline, aniline-Ar, and aniline-Ar_2. These were obtained using two-color photoionization, where the probe laser was above the ionization threshold and the pump laser frequency was scanned. Signal from each of the respective mass channels was recorded and is consistent with previously published results.[3,4,18] An important point to note is the shift of the An–Ar and An–Ar_2 origin bands, 53 and 107 cm^{-1}, respectively, from those of the monomer. The additivity of the shifts is well documented in this, and similar $n=1$ and $n=2$ systems, and indicates that the position of each Ar atom is the same, relative to the An monomer. It is well established in An–Ar that the Ar position is located above the π system,[5,16] and so the An–Ar_2 complex is expected to have an Ar on each side of the ring in a similar position.

The MATI spectra are obtained by pumping through the respective origins of each complex, scanning the probe laser above the ionization potential, and gating on the mass chan-

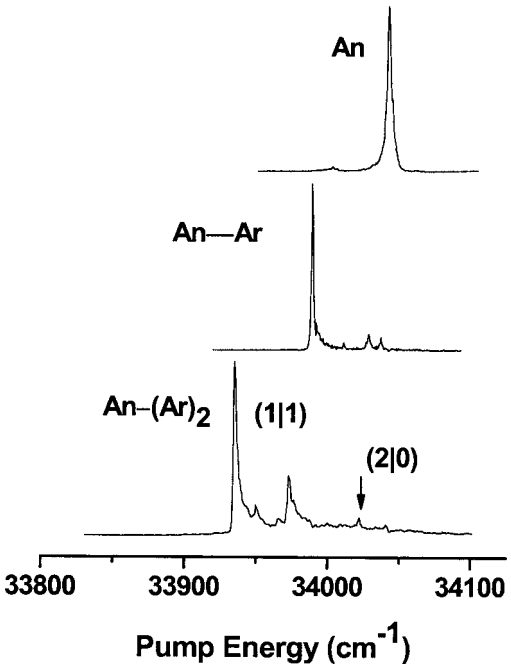

FIG. 2. Mass resolved MPI spectra for the S_1 origin region of aniline (An) and aniline complexes with one and two argon atoms. The mass-gated spectra were obtained by scanning the pump laser as indicated and probing with a fixed laser energy which exceeds the ionization potential. The $An-Ar_2$ complex has been assigned to have two conformers which are indicated by the $(1|1)$ and $(2|0)$ designations.

nels of interest. Figure 3 shows the MATI spectrum of each complex near the ionization threshold. The vibronic patterns for each complex are quite unique and have been analyzed in detail previously.[18] At the ionization threshold no MATI signal is detected in the lower mass channels. As the MATI probe is scanned to higher energy, a signal is observed in the channel of the dissociation product (An^+ for the An–Ar complex and both An^+-Ar and An^+ for $An-Ar_2$). The appearance of the dissociation product then marks the dissociation

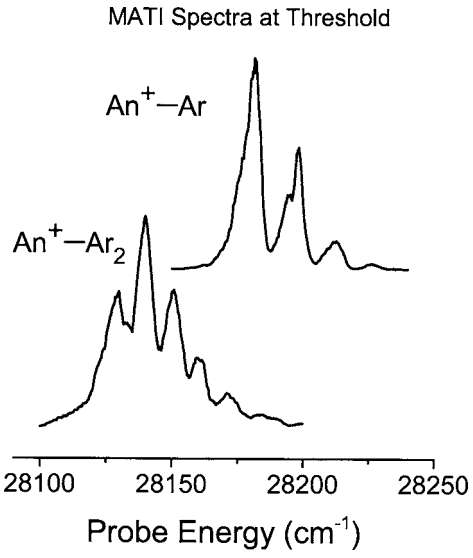

FIG. 3. MATI spectra of the An–Ar and $An-Ar_2$ complexes obtained by pumping the respective S_1 origins (33 987 and 33 932 cm^{-1}) and scanning the probe in the region of the ionization thresholds. The corresponding threshold for the aniline monomer (not shown) is 28 241 cm^{-1}.

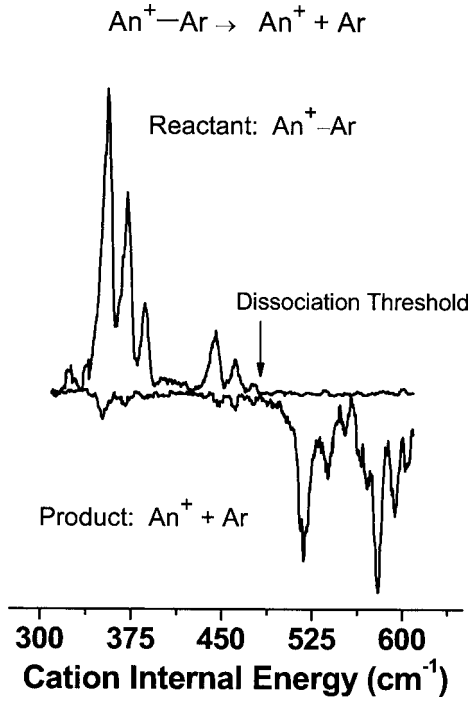

FIG. 4. MATI spectra obtained by pumping the An–Ar S_1 origin and then scanning the probe above the ionization threshold as indicated. The x axis is relative to the threshold at 28 181 cm^{-1}. The positive going spectrum is the signal obtained by gating on the reactant An^+-Ar mass and the negative going spectrum is the signal gating on the dissociation product An^+. The negative going spectrum has been inverted for clarity of presentation.

threshold and can be used to measure the cation complex binding energy. This technique has been well documented by Krause and Neusser.[21]

A. $An^+-Ar \rightarrow An^+ + Ar$

Figure 4 shows the MATI spectrum of the $An-Ar_1$ complex at higher energy in the cation, again pumping through the S_1 origin, and plotting signal for both the complex $(An-Ar^+)$ channel and the monomer (An^+) channel (the product is shown as a negative going spectrum so as to be clearly identified compared to the reactant). The x axis represents the total energy above the complex ionization threshold for An–Ar (62 168 cm^{-1}), and thus directly represents the total vibrational energy. The point at which the complex mass signal disappears is between 480 and 510 cm^{-1}. Below 480 cm^{-1} there are three bands which show intensity in both the complex and monomer channels, with the monomer increasing in intensity relative to the complex for each band. The presence of intensity in the monomer channel just below the actual threshold has been documented and explained by Gretner *et al.*[25] as being due to coupling to lower Rydberg states that occurs when large voltage extraction pulses are used, such as the ~900 V/cm employed in our experiment. The threshold for disappearance of the complex signal is not affected by the field and thus is used as a more reliable value to determine the dissociation energy. In this particular case it appears as if the signal disappears at 480 cm^{-1}. However, the overall signal level in this region is quite small (as evidenced by a small signal in the product channel) and so the range of uncertainty of dissociation extents to ~510 cm^{-1}, where the

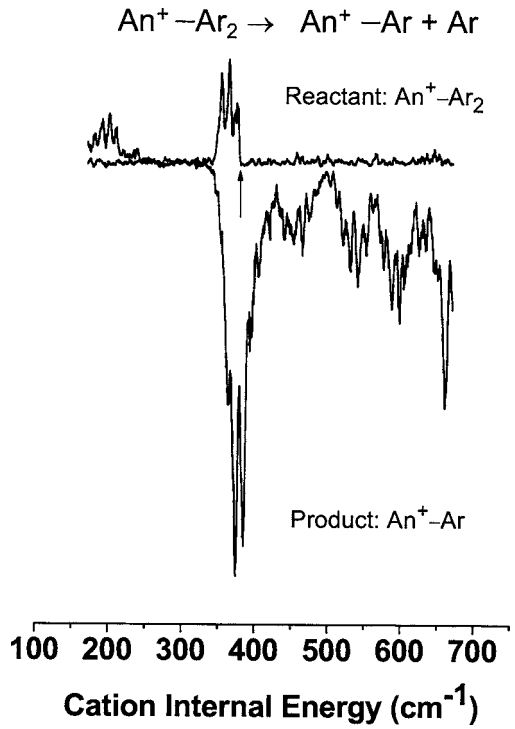

FIG. 5. MATI spectra obtained by pumping the $An-Ar_2$ S_1 origin and then scanning the probe above the ionization threshold as indicated. The x axis is relative to the threshold at 28 129 cm^{-1}. The positive going spectrum is the signal obtained by gating on the reactant An^+-Ar_2 mass and the negative going spectrum is the signal gating on the dissociation product An^+-Ar.

product signal picks up with no observable reactant signal. Therefore, the An^+-Ar dissociation energy is determined to be 495 ± 15 cm^{-1}. Further evidence that the monomer ion signal originates from the dissociation of the complex is the appearance of the spectral features at 520 and 575 cm^{-1} in the figure. These bands have the characteristic pattern associated with the An–Ar MATI spectrum (Fig. 3) and thus confirm the parentage. The binding energy in the S_1 and S_0 neutral states can be obtained by combining this cation binding energy with the measured spectral shifts. The error in these shifts is negligible compared to the uncertainty in the cation binding energy and thus the errors are of the same magnitude. This results in approximate values of 440 ± 15 cm^{-1} for S_1 and 380 ± 15 cm^{-1} for S_0.

One point to emphasize is that after laser excitation there is a ~ 25 μs delay until the extraction pulse is applied. Thus it is unlikely that metastable complexes would give an artificially high dissociation threshold. This is always a concern in S_1 excited state measurements, where the short excited state lifetime might prevent the true threshold from being observed.

B. $An^+-Ar_2 \rightarrow An^+-Ar+Ar$

Figure 5 shows the MATI spectrum of the $An-Ar_2$ complex at higher energy in the cation, again pumping through the S_1 origin, and plotting signal for both the complex (An^+-Ar_2) parent channel and the expected product channel (An^+-Ar). The onset for dissociation is quite clear in this case as indicated by the arrow in the figure, yielding a dissociation energy of 380 ± 5 cm^{-1}. It is fortuitous that the dissociation occurs within the profile of a rather strong band, significantly reducing the uncertainty in the dissociation threshold. Again, the product signal appears before complete loss of the parent, but we use the disappearance of the reactants as the precise dissociation threshold. By contrast the lower energy band at ~ 200 cm^{-1} shows only signal in the parent channel and no sign of dissociation.

The value for the dissociation energy for An^+-Ar_2, 380 cm^{-1}, is quite surprising because it is smaller by 115 cm^{-1} than that for loss of Ar in An^+-Ar. One might argue that this is not completely surprising because the second Ar may have a significantly different position than that of the Ar in An^+-Ar with different interactions and thus a different binding energy. However, there is strong evidence that this is not the case. First, as mentioned above, the spectral shifts from S_0 to S_1 are completely additive for each of the argons. The additivity is also present in the shifts from S_1 to the cation, being 60 and 113 cm^{-1}, respectively. If the Ar binding sites are equivalent in the neutral, then the optical transitions to the cation are not able to access conformations which are significantly different due to the Franck-Condon principle. In the neutral *para*-difluorobenzene-Ar_2 complex it was shown that the two π bound Ar atoms had almost identical binding energies with very small three body effects.[26]

C. $An^+-Ar_2 \rightarrow An^+ + 2Ar$

The complete dissociation of An^+-Ar_2 was measured by monitoring the MATI signal in the An^+-Ar and An^+ mass channels when pumping the $An-Ar_2$ S_1 origin and scanning the probe ~ 1000 cm^{-1} above the ionization threshold. In this region loss of at least one Ar is assumed and the threshold for dissociation of the second Ar is sought. Figure 6 shows the resulting spectrum with a clear threshold for loss of the second Ar observed at ~ 1020 cm^{-1}. Below the second dissociation threshold the MATI signal appears in the An^+-Ar channel. Again confirmation that the signal is due to the initially pumped $An-Ar_2$ is seen in the spectral structure of the peaks at 830 and 1020 cm^{-1}, which are indicative of the $An-Ar_2$ complex. The peak at 1020 cm^{-1} is broadened, but has the overall shape of the Ar_2 complex peaks. The broadening could be due to the Rydberg coupling mechanism mentioned above.[25]

The threshold for loss of the second Ar occurs within the profile of a strong band and so one might expect a sharp threshold. However, this is not observed and is likely due to the fact that the loss of the first Ar can take place with varying degrees of kinetic energy loss, therefore the remaining products have a distribution of internal energy. The net effect is that some Ar_2 molecules above threshold for loss of both Ar will not fully dissociate. Belm and Lawrence[26] have shown that for similar complexes the kinetic energy release is modest, and so the ~ 40 cm^{-1} width of the dissociation threshold is not unexpected here.

Given this uncertainty in the exact position of complete dissociation, we assign the energy as 1020 ± 15 cm^{-1}. This value is then within experimental uncertainty of twice the

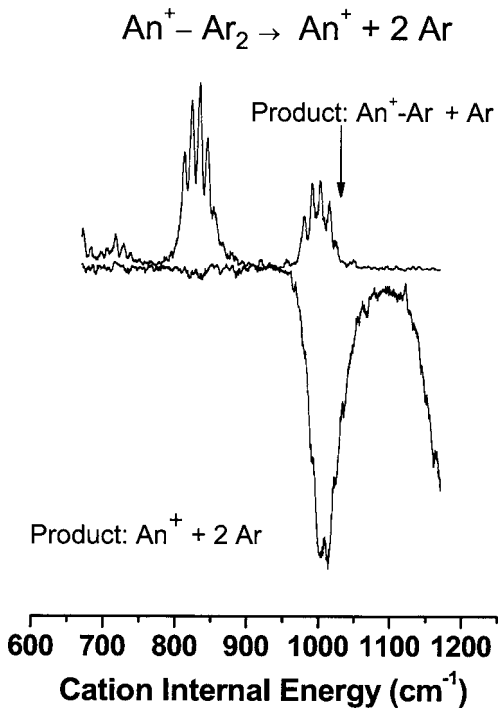

FIG. 6. MATI spectra obtained by pumping the An–Ar_2 S_1 origin and then scanning the probe above the ionization threshold as indicated. The x axis is relative to the threshold at 28 129 cm^{-1}. In this case the entire spectral range is above the energy for loss of at least one argon atom. The positive going spectrum is the signal obtained by gating on the first product appearing (An^+–Ar), and the negative going spectrum is the signal gating on the fully dissociated product An^+.

dissociation energy of An^+–Ar, consistent with the additivity rules for the spectral shifts, suggesting that three body effects on the binding energy are modest.[26,27]

D. $An^+–Ar_2(2|0) \rightarrow An^+–Ar+Ar$

Brechignac and co-workers,[3,19,28] had identified a second conformation for the neutral An–Ar_2 which they designated as (2|0). This nomenclature for clusters with multiple Ar atoms indicates the number of Ar on each side of the phenyl ring by the numbers on either side of the vertical bar. The $n=2$ complexes discussed above, with one Ar on each side, is designated as (1|1). The (2|0) neutral species was assigned to the resonant transition at 34 019 cm^{-1} and was identified as a distinct isomer by the shift of its ionization potential. Note that the S_1 transition is shifted 87 cm^{-1} to the *blue* of the $n=2$, (1|1) S_1 resonance. This violates the additivity rule and indicates that the two Ar atoms are in different positions. Using pairwise atom-atom interaction potentials Parneix *et al.*[19] assigned the (2|0) structure as having both Ar atoms on the same side, with one being more centered on the phenyl ring and the other being displaced to the side toward the amine group.

This weak transition is indicated in Fig. 2 and a MATI spectrum was taken pumping through this resonance, Fig. 7. A broad feature was observed near the ionization threshold making assignment of an exact threshold difficult. We assign a value of 27 898 cm^{-1} which compares well to the value of 27 908 cm^{-1} determined by Douni *et al.* using photoionization efficiency curves.[28] Due to a weak signal the cation

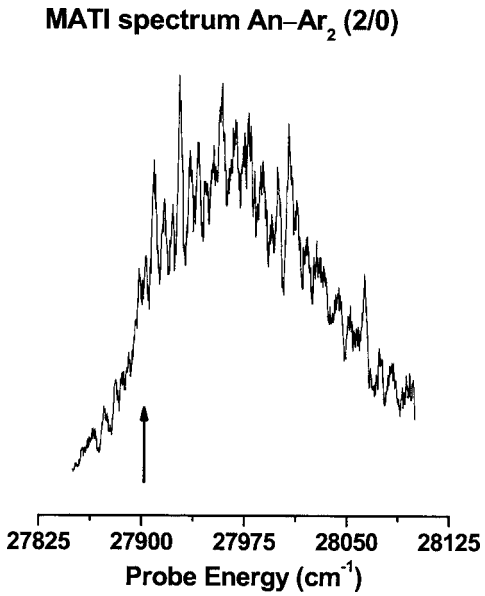

FIG. 7. MATI spectrum obtained by pumping the An–Ar_2 cluster in the (2|0) conformation (34 019 cm^{-1}) and scanning the probe in the region of the ionization threshold as indicated. The onset here is quite broad and the arrow represents an estimate of the ionization threshold.

dissociation threshold of this isomer could not be determined. The notable point about this result is that the IP of this isomer is 144 cm^{-1} less than the (1|1) species. This conformation will be discussed further below.

IV. CALCULATIONS

With current *ab initio* methods it is possible to calculate the structure and binding energies of weakly bound clusters with reasonable accuracy. These methods have been successfully applied to the An–Ar neutral[16,20] and similar weakly bound systems.[29–31] Solca and Dopfer[7] have also done calculations on the An–Ar cation system, focusing on the Ar hydrogen bonding configuration. Using the UMP2 method with a 6311G(2*df*,2*dp*) basis set, they determined that both the π-bonded and the H-bonded configurations are stable minima, but that the latter is the more stable global minima by approximately 60 cm^{-1}. As they stated this basis set is limiting and the overall binding energies were expected to be underestimated. Our interest was in calculating accurate bonding energies and this requires a larger basis set and different methods then applied in their study. All calculations were performed using the GAUSSIAN 03 computational package.[32] Makarewicz has performed calculations on the closely related *p*-difluorobenzene-Ar cation complex and we follow his approach with some modification.[30] For neutral clusters a successful approach has been MP2 calculations using the Dunning aug-cc-pVTZ basis set[33] with the counterpoise method used to correct for basis set superposition error (BSSE).[34] In addition frequency calculations are employed to determine the zero-point energy contribution to the dissociation energy. For the cation, however, there is a problem with the MP2 method in that UMP2 must be used which results in spin contamination. If one does an optimization with UMP2 an incorrect structure is obtained for the An cation and therefore a possible error in the complex structure

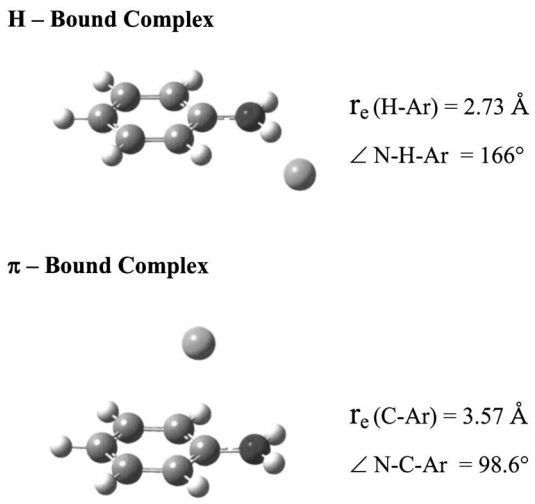

FIG. 8. Structural minima of An^+-Ar as determined by counterpoise corrected ROMP2 calculations using an aug-cc-pVDZ basis set. The monomer cation was fixed at the geometry calculated using B3LYP density functional theory with the same basis set.

and energy can result. The approach we have taken is to do an optimization of the An cation using the B3LYP density functional method using the aug-cc-pVDZ basis set and then freezing this geometry throughout the remaining calculations. The error introduced by not allowing the An cation to relax upon complexation is expected to be minimal. To test this hypothesis complete optimizations at the UMP2 level were performed and the binding energy results were found to be similar to the frozen An calculations.

Using this frozen An cation structure, optimizations were performed on the An–Ar complex using UMP2 and the aug-cc-pVDZ basis set. A number of starting configurations were chosen in order to find possible multiple minima on the cation complex potential energy surface. Two low lying minima were found, the π-bound and H-bound structures which are shown in Fig. 8. To get the final binding energy a single point calculation was performed at each of the minimum structures using a larger basis set, aug-cc-pVTZ, and applying the counterpoise correction. The zero point energy was obtained by calculation of only the intermolecular modes with the larger, aug-cc-pVTZ basis set. These modes were in good agreement with the previously experimentally measured intermolecular vibrational frequencies in the cation complex.[18] The intramolecular modes, particularly in the H-bonded configuration, could very well be influenced by the Ar atom binding but this effect was not taken into account.

The UMP2 calculations are consistent with previously published results[7] and reveal that the minimum structure in the neutral, with the Ar above the π system, is only the second lowest energy conformation in the cation. The lowest energy conformation has the Ar in a H-bonding arrangement with the N–H bond, in the plane of the An cation. The in-plane Ar H bond is not linear but has a N–H–Ar bond angle of 166°, with the Ar displaced toward the An ring. The calculated binding energy for the π-bound structure is $\sim 500\ cm^{-1}$, in excellent agreement with experiment, but the H-bound species has a binding energy of $517\ cm^{-1}$, not as stable as expected from the experimental measurements. Given the concern about spin contamination, we proceeded to additional calculations using ROMP2 and UMP3 methods, both using the aug-cc-pVTZ basis set. These are summarized in Table I along with the UMP2 results. The UMP3 calculations predict a much different stabilization between the π- and H-bound structures but appear to underestimate the binding energy. The ROMP2 calculations give a stronger interaction but similar binding energies for both isomers. Different optimizations of the Ar position were tried using ROMP2 and counterpoise corrected optimizations,[31,35] but the resulting bond energies did not change significantly.

TABLE I. Summary of calculated and experimental An^+-Ar binding energies. All calculation used the aug-cc-pVTZ basis set with fixed aniline cation structure and counterpoise BSSE correction.

	π-bound cation complex		H-bound cation complex	
	$D_e\ (cm^{-1})$	$D_0\ (cm^{-1})$[a]	$D_e\ (cm^{-1})$	$D_0\ (cm^{-1})$[a]
UMP2	548	497	575	517
ROMP2	663	612	652	609
UMP3	349	297	518	459
Expt.[b]	···	495 ± 15	···	630 ± 20

[a]Zero point energy determined from a UMP2 aug-cc-pVTZ frequency calculation of the intermolecular modes.
[b]Measured values reported in this work.

V. DISCUSSION

The above experimental measurement of the π bound Ar binding energy in the cation is $495 \pm 15\ cm^{-1}$. Combining this with the spectral shifts leads to values of 435 ± 15 and $380 \pm 15\ cm^{-1}$ for S_1 and S_0, respectively. The cation binding energy and the derived neutral values are not in agreement with the published values of Piest *et al.*[6] who measured the dissociation using infrared photodissociation in the cation. They bracketed the dissociation as occurring between the vibrational states of 442 and $386\ cm^{-1}$, which is considerably below our measured value. We have no explanation for this discrepancy. Metastability of states above the dissociation limit is not likely to explain the difference because both experiments have microseconds time scale delay times in which the dissociation can take place. In our experiments the delay time was 25 μs. Nimlos *et al.*[4] bracketed the S_1 binding energy between 442 and $460\ cm^{-1}$. The lower limit is slightly below our value of $435\ cm^{-1}$, but the discrepancy could easily be explained by metastability of the $435\ cm^{-1}$ vibration in S_1 state due to the less than 10 ns excited state lifetime. There is excellent agreement between our measured and calculated values; however, this needs to be viewed with caution as discussed below.

Dissociation of the An^+-Ar_2 complex was the most surprising measurement, yielding a low value of $380\ cm^{-1}$ for loss of one Ar. We have determined that this value is indeed loss of a π bonded Ar, but in fact involves rearrangement of the remaining Ar to the lower energy H-bonded configuration. Figure 9 shows the relevant energy level diagram. The initial configuration of the An^+-Ar_2 complex is two π bound Ar's as determined by the geometry of the neutral and the

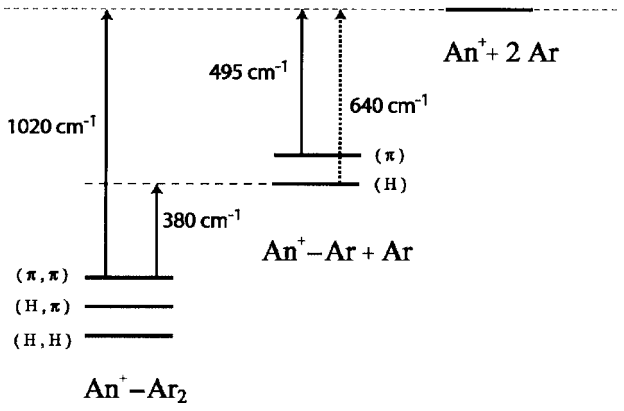

FIG. 9. Schematic energy level diagram for An^+-Ar and An^+-Ar_2 dissociation pathways. The solid vertical arrows indicate the experimentally measured values. The dashed arrow, which is the binding energy of the H-bonded species, indicates an inferred value using the other known quantities.

vertical nature of the optical excitation. However, Ishiuchi *et al.*,[2] in the closely related phenol$^+$-Ar system, observed conformer "switching"[36] in which the initially created π bound Ar was observed to rapidly rearrange to the more stable H-bonded configuration, with essentially no barrier. Solca and Dopfer[13] have made infrared measurements of the phenol$^+$-Ar system and see both the π-bound and H-bound complexes but calculate a relatively small barrier between them. In our experiment we postulate that upon excitation the $An-Ar_2$ complex rearranges so that at least one of the Ar is H bonded. This has the effect of releasing additional energy in the cluster which can then contribute to the dissociation energy of the π-bound Ar. Essentially, the An^+-Ar H-bonded species provides an additional, lower, exit channel for the dissociation of the π-bonded An^+-Ar_2. The measured 380 cm^{-1} then represents the threshold for this channel.

The energetics of Fig. 9 are further refined by the measurement of the dissociation energy for both Ar atoms. This value is 1020 cm^{-1} as determined above and indicated on the figure. Any rearrangements to the H-bonded configuration are of no consequence to this measurement because it is only the initial (two π bound Ar) and final (bare An^+ and two argon atoms) states which determine the energetics. This is also true for loss of one π bound Ar from An^+-Ar, the value of which is also included in the diagram (495 cm^{-1}). From the energetics of Fig. 9 one can determine the binding energy of the H-bound Ar. It is just the dissociation energy of both π bound Ar atoms, 1020 cm^{-1}, minus the appearance of the H-bound product channel, 380 cm^{-1}, yielding a H-bound binding energy of 640 ± 20 cm^{-1}. Another way of viewing this is that the appearance of the H-bound dissociation channel is 380 cm^{-1}, which is 115 cm^{-1} below the π bound dissociation energy of 495 cm^{-1}, thus the H-bound configuration has a binding energy of $495+115=610 \pm 20$ cm^{-1}. The discrepancy in these values is within experimental error but the first approach is more reliable because it does not make any assumptions about three-body effects. The substantially more stable H-bound configuration is consistent with the results of Solca and Dopfer,[7] who observed this as the dominant configuration when the complex was created starting with the aniline cation, rather than the neutral aniline.

The agreement between calculation and experiment is mixed. The UMP2 calculations are in excellent agreement with regard to the experimentally measured binding energy of the Ar^+-Ar π-bound species, but do not give a significantly more stable H-bound structure as measured. The ROMP2 results are similar, but with a somewhat stronger bond energy. The MP3 calculations yield a difference in stability between π and H bound which is in agreement with experiment, but underestimates the overall binding energy. Our experimental extrapolation of the neutral S_0 binding energy is ~ 380 cm^{-1}. This is consistent with the calculation of Makarewicz for the neutral π-bound complex.[16] Using a higher level of theory [CCSD(T)] and larger basis set they obtained a neutral binding energy, $D_0=387$ cm^{-1}.

It is possible that the calculations of the H-bound species converge differently with regard to level of theory and basis set and so require more sophisticated calculations.[31] Our current resources make the CCSD(T) calculations prohibitive. We also have considered the possibility that our interpretation of the π-bound exit channel is flawed or lacking but have not found a more reasonable explanation. Whether the lower exit channel is the π-bound geometry is not determined in the experiment but searches of the An^+-Ar surface have not revealed any other low energy minima. Also the IR experiments of Solca and Dopfer[7] confirm that the lowest energy cation conformation is H bound.

Interpretation of the results for the (2|0) cluster presented above is difficult because we were unable to measure the dissociation energy. However, the significant redshift of the ionization potential would indicate that one of the Ar atoms is H bound in the cation, and since it is optically accessible this suggests that the neutral is also in a H-bound configuration. Calculations do show that the second lowest (2|0) neutral configuration has one Ar in a near H-bonding configuration and so it may be reasonable to assume that the optical transition to the cation does produce the H-bonding cation. The broad MATI peak at threshold indicates a significant geometry change. In fact it is not clear that the MATI spectrum identifies the threshold or perhaps is just accessing the Franck-Condon region that could be above the real IP.

VI. CONCLUSIONS

MATI spectroscopy is used to determine the Ar binding energies in the cations An^+-Ar and An^+-Ar_2. By combining these data with the measured spectral shifts, the binding energies in the S_1 and S_0 states are also obtained. The value for An^+-Ar is not in agreement with the results of Piest *et al.*,[6] but is in reasonable agreement with the results of Nimlos *et al.*[4] determined in the S_1 state.

Although the H-bonded species is not directly created in the experiments, its binding energy is obtained indirectly and represents the first determination for this configuration. The results confirm that this species is the most stable configuration in the cation, consistent with experiments which create

the An^+-Ar starting with the monomer cation. These results are consistent with, and compliment, the recently published results on phenol$^+$-Ar.[2]

The MATI technique is also applied to measure the loss of two Ar atoms from An^+-Ar_2, and the results reveal that each Ar has the same binding energy, consistent with their equivalent π-bonding sites. The sensitivity suggests that measurements on even larger clusters would be possible.

ACKNOWLEDGMENTS

We would like to thank Professor George Petersson of Wesleyan University for his expert advice on performing the GAUSSIAN 03 calculations. We gratefully acknowledge the computational resources provided on the Wesleyan University computer cluster supported by the NSF under Grant No. CNS-0619508.

[1] R. Leist, J. A. Frey, and S. Leutwyler, J. Phys. Chem. A **110**, 4180 (2006); R. Leist, J. A. Frey, P. Ottiger, H.-M. Frey, S. Leutwyler, R. A. Bachorz, and W. Klopper, Angew. Chem., Int. Ed. **46**, 7449 (2007); S. Ishiuchi, M. Sakai, Y. Tsuchida, A. Takeda, Y. Kawashima, M. Fujii, O. Dopfer, and K. Muller-Dethlefs, Angew. Chem., Int. Ed. **44**, 6149 (2005).
[2] S.-I. Ishiuchi, M. Sakai, Y. Tsuchida, A. Takeda, Y. Kawashima, O. Dopfer, K. Muller-Dethlefs, and M. Fujii, J. Chem. Phys. **127**, 114307 (2007).
[3] P. Hermine, P. Parneix, B. Coutant, F. G. Amar, and P. Brechignac, Z. Phys. D: At., Mol. Clusters **22**, 529 (1992).
[4] M. R. Nimlos, M. A. Young, E. R. Bernstein, and D. F. Kelley, J. Chem. Phys. **91**, 5268 (1989).
[5] W. E. Sinclair and D. W. Pratt, J. Chem. Phys. **105**, 7942 (1996).
[6] H. Piest, G. von Helden, and G. Meijer, J. Chem. Phys. **110**, 2010 (1999).
[7] N. Solca and O. Dopfer, Eur. Phys. J. D **20**, 469 (2002).
[8] K. Muller-Dethlefs, M. Sander, and E. W. Schlag, Chem. Phys. Lett. **112**, 291 (1984); C. E. H. Dessent and K. Muller-Dethlefs, Chem. Rev. (Washington, D.C.) **100**, 3999 (2000); E. W. Schlag, *ZEKE Spectroscopy* (Cambridge University Press, Cambridge, 1998); K. Mullerdethlefs, O. Dopfer, and T. G. Wright, Chem. Rev. (Washington, D.C.) **94**, 1845 (1994).
[9] L. C. Zhu and P. Johnson, J. Chem. Phys. **94**, 5769 (1991).
[10] H. J. Neusser and H. Krause, Chem. Rev. (Washington, D.C.) **94**, 1829 (1994); J. D. Pitts and J. L. Knee, J. Chem. Phys. **108**, 9632 (1998).
[11] X. Zhang, J. D. Pitts, R. Nadarajah, and J. L. Knee, J. Chem. Phys. **107**, 8239 (1997).
[12] T. Pino, S. Douin, N. Boudin, and P. Brechignac, Chem. Phys. Lett. **419**, 356 (2006).
[13] N. Solca and O. Dopfer, J. Mol. Struct. **563**, 241 (2001).
[14] N. Solca and O. Dopfer, Chem. Phys. Lett. **369**, 68 (2003).
[15] E. J. Bieske, A. S. Uichanco, M. W. Rainbird, and A. E. W. Knight, J. Chem. Phys. **94**, 7029 (1991); K. Kimura, J. Electron Spectrosc. Relat. Phenom. **108**, 31 (2000); J. G. Jackel and H. Jones, Chem. Phys. **247**, 321 (1999); X. Zhang and J. L. Knee, Faraday Discuss. **97**, 299 (1994); M. Takahashi, H. Ozeki, and K. Kimura, J. Chem. Phys. **96**, 6399 (1992); T. Pino, P. Parneix, S. Douin, and P. Brechignac, J. Phys. Chem. A **108**, 7364 (2004); S. Douin, P. Parneix, F. G. Amar, and P. Brechignac, J. Phys. Chem. A **101**, 122 (1997).
[16] J. Makarewicz, J. Phys. Chem. A **111**, 1498 (2007).
[17] J. M. Smith, X. Zhang, and J. L. Knee, J. Chem. Phys. **99**, 2550 (1993).
[18] Z. Xu, J. M. Smith, and J. L. Knee, J. Chem. Phys. **97**, 2843 (1992).
[19] P. Parneix, P. Brechignac, and F. G. Amar, J. Chem. Phys. **104**, 983 (1996).
[20] I. Lopez-Tocon, J. C. Otero, M. Becucci, G. Pietraperzia, and E. Castellucci, Chem. Phys. **249**, 113 (1999).
[21] H. Krause and H. J. Neusser, J. Chem. Phys. **97**, 5923 (1992); H. Krause and H. J. Neusser, J. Chem. Phys. **99**, 6278 (1993).
[22] S. Basu and J. L. Knee, J. Chem. Phys. **120**, 5631 (2004); J. D. Pitts, S. Basu, and J. L. Knee, J. Chem. Phys. **113**, 1857 (2000); J. D. Pitts, J. L. Knee, and S. Wategaonkar, J. Chem. Phys. **110**, 3378 (1999); Q. L. Gu, S. Basu, and J. L. Knee, J. Phys. Chem. A **111**, 1808 (2007).
[23] H. J. Dietrich, R. Lindner, and K. Mullerdethlefs, J. Chem. Phys. **101**, 3399 (1994).
[24] W. C. Wiley and I. H. Mclaren, Rev. Sci. Instrum. **26**, 1150 (1955).
[25] T. L. Grebner, P. von Unold, and H. J. Neusser, J. Phys. Chem. A **101**, 158 (1997).
[26] S. M. Bellm and W. D. Lawrance, Chem. Phys. Lett. **368**, 542 (2003).
[27] P. Hobza, O. Bludsky, H. L. Selzle, and E. W. Schlag, Chem. Phys. Lett. **250**, 402 (1996).
[28] S. Douin, S. Piccirillo, and P. Brechignac, Chem. Phys. Lett. **273**, 389 (1997).
[29] J. Makarewicz, J. Chem. Phys. **123**, 44307 (2005); **122**, 114312 (2005); **124**, 44310 (2006); **124**, 84310 (2006).
[30] J. Makarewicz, J. Chem. Phys. **123**, 154302 (2005).
[31] K. Muller-Dethlefs and P. Hobza, Chem. Rev. (Washington, D.C.) **100**, 143 (2000).
[32] M. J. T. Frisch, G. W. Trucks, H. B. Schlegel *et al.*, GAUSSIAN 03, Gaussian, Inc., Pittsburgh, PA, 2003.
[33] T. H. Dunning, J. Phys. Chem. A **104**, 9062 (2000).
[34] H. B. Jansen and P. Ross, Chem. Phys. Lett. **3**, 140 (1969); S. F. Boys and F. Bernardi, Mol. Phys. **19**, 553 (1970).
[35] S. Simon, M. Duran, and J. J. Dannenberg, J. Chem. Phys. **105**, 11024 (1996).
[36] O. Dopfer, Z. Phys. Chem. **219**, 125 (2005).